Electric Field-directed Cell Shape Changes, Displacement, and Cytoskeletal Reorganization Are Calcium Dependent

Edward K. Onuma and Sek-Wen Hui

Department of Biophysics, Roswell Park Memorial Institute, Buffalo, New York 14263

Abstract. C3H/10T1/2 mouse embryo fibroblasts were stimulated by a steady electric field ranging up to 10 V/cm. Some cells elongated and aligned perpendicular to the field direction. A preferential positional shift toward the cathode was observed which was inhibited by the calcium channel blocker D-600 and the calmodulin antagonist trifluoperazine. Rhodamine-phalloidin labeling of actin filaments revealed a field-induced disorganization of the stress fiber pattern, which was reduced when stimulation was conducted in calcium-depleted buffer or in buffer containing calcium antagonist $CoCl_2$, calcium channel blocker D-600, or calmodulin antagonist trifluoperazine. Treatment with calcium ionophore A23187 had similar effects, except that the presence of D-600 did not reduce the stress fiber disruption.

The calcium-sensitive photoprotein aequorin was used to monitor changes in intracellular-free calcium. Electric stimulation caused an increase of calcium to the micromolar range. This increase was inhibited by calcium-depleted buffer or by $CoCl_2$, and was reduced by D-600. A calcium-dependent mechanism is proposed to explain the observed field-directed cell shape changes, preferential orientation, and displacement.

DIRECTED and coordinated cell movement plays a determining role during embryonic development and wound healing. In motile tissue cells such as fibroblasts and epithelial cells, natural movement is generated by localized instabilities of the cell periphery that allow one or more leading lamellae to extend outward (19). The propulsive forces responsible for lamellar extension are generated by a mechanism believed to be regulated by calcium (5, 34), and the direction of movement is dictated by the broadest and strongest leading lamella (1, 43). Several factors are believed to direct cell shape changes and movement. These include intrinsic factors programmed within the cell as well as extrinsic influences such as chemotaxis, galvanotaxis (electric field directed), contact guidance, haptotaxis, and contact inhibition (43).

Recently, the role played by electric fields has attracted the research efforts of a number of investigators (30). This influence was first studied by Verworn in 1889 (44), and many of the related early works were reviewed by Lund in 1947 (24). In 1966 Jaffe demonstrated that developing *Fucus* zygotes in a multi-cell system generates endogenous transcellular currents (22). The need for spatial and temporal resolution led to the development of the ultrasensitive vibrating probe technique (23), and since then numerous laboratories have been able to measure ionic current patterns in developing embryonic systems (29) and at sites of injury (7). In the past few years, there has also been a growing interest in the effects of an applied electric field on cells in culture (38).

In an earlier work, we observed the electric field-induced cell shape changes and preferential alignment of C3H/10T1/2 mouse embryo fibroblasts (47). Subsequently, we provided evidence showing that the response was mediated through an influx of calcium across the plasma membrane (possibly localized) and that the calcium-binding protein calmodulin may be involved (32). We report here a preferential positional shift of the cells toward the cathode. Using the photoprotein aequorin and the actin-binding probe rhodamine-phalloidin, we observed an electric field-induced increase in intracellular-free calcium levels and a disruption of cytoskeletal stress fiber organization. All responses were inhibited by blocking calcium influx across the plasma membrane. We propose a mechanism to explain the observed field-directed cell shape changes, preferential orientation, and displacement.

Materials and Methods

Cell Culture

Establishment and characterization of the C3H/10T1/2 cell line have been previously detailed (37), and culturing procedures were described in earlier works (32, 47). In most cases the cells were plated onto acid-washed, sterile glass coverslips (18 × 18 mm) attached to the bottom of 60-mm culture dishes, and allowed to spread for 48 h. For each experiment, the cell density was maintained at a subconfluent stage, and ~80% of the cells were well spread and 20% were spindle shaped.

Electric Field Stimulation

The apparatus used for electric field stimulation was based on the design described by Poo et al. (36). A 22 × 2 × 0.2-mm trough was formed be-

tween coverslips on a glass slide. At either end of the trough was a fluid reservoir, and two 10-cm-long 2% agar bridges connected the two reservoirs to platinum electrodes immersed in buffer. The electric field was provided by a voltage-regulated power supply and continuously monitored by two platinum tips immersed at the ends of the trough. All experiments were carried out at room temperature.

Normally, the coverslips containing the cells were taken from the culture medium and rinsed once in buffer for 5 min, then incubated in their respective experimental solution for 5 min before field application (in some experiments culture media was used during field application). In the case of D-600 treatment, incubation time was 15 min. The coverslips were then sealed cell-side down onto the trough with vacuum grease. At a typical field strength of 10 V/cm, the current through the trough was ~2.5 mA and the steady-state temperature after 2 min was ~27°C.

Cell Scoring

Cell viability immediately after experiments was determined by the trypan blue (diluted 1:1,000) exclusion test, and for each experimental condition >100 cells were scored at a magnification of 100. To assess the effects of the scrape-loading technique on cell growth, cells were scraped in the presence or absence of the aequorin stock solution and then replated. 1, 2, and 3 d later, cultures were collected by incubation with 0.25% trypsin (Gibco, Grand Island, NY), and total cell number was determined on a Coulter counter (model ZBI; Coulter Electronics, Inc., Hialeah, FL).

Cell shape changes, orientation, and displacement were measured by time-lapse photomicroscopy. The same field of view was identified by scratch marks made on the glass coverslips. To assess cell shape changes, the cells were scored as being either flat or spindle-shaped before and after each experiment. The asymmetry index (32, 47) was used to determine preferential orientation of the spindle-shaped cells. A blind scoring system minimized measuring bias.

Photomicrographic images of the same field of view were taken every 10 min for up to 1 h, and the position of each cell nucleus was recorded for each time interval. The total displacement of each cell was summed and divided by the time period to calculate the average speed of the population. The method to determine directional migration was based on the one used by Erickson and Nuccitelli (15). Briefly, a line was drawn from the origin to the final position of each cell nucleus in the time period. The net displacement and the cosine of the angle formed between this line, and the direction of the electric field (an arbitrary baseline in the case of control conditions) were measured. The net displacement was multiplied by the directional cosine to yield a vectorial displacement. The sum of the vectorial displacements divided by the total number of motile cells scored gives an indication of preferential cell displacement along the field direction.

Chemicals

Normal PBS (137 mM NaCl, 9.6 mM Na_2HPO_4, 0.5 mM $MgCl_2$, 2.6 mM KCl, 1.5 KH_2PO_4, and 0.9 mM $CaCl_2$ at pH 7.4) or normal balanced salt solution (125 mM NaCl, 5 mM KCl, 3.8 mM $CaCl_2$, 2.5 mM $MgCl_2$, and 5 mM Tris at pH 7.4) were used as the medium for most experiments. Calcium-depleted PBS was prepared with no added calcium and supplemented with 0.5 mM EGTA and 2 mM $MgCl_2$. Modified balanced salt solution to hyperpolarize the plasma membrane (14) consisted of 130 mM sodium gluconate in place of NaCl and KCl. Cobalt chloride was dissolved in balanced salt solution at a concentration of 10 mM. The calcium channel blocker D-600 was synthesized by Dr. David Triggle (Department of Biochemical Pharmacology, State University of New York at Buffalo) and obtained through Dr. Frederick Sachs (Department of Biophysical Sciences, State University of New York at Buffalo). It was dissolved in deionized distilled water and added to the medium up to a concentration of 1 μM. The calmodulin inhibitor trifluoperazone or the ionophore A23187 (Sigma Chemical Co., St. Louis, MO) was dissolved in 95% ethanol and added to the medium to concentrations of 5 and 4 μM, respectively. (Ethanol concentration was maintained at 0.5% [vol/vol].) Cytochalasin D (Sigma Chemical Co.) was dissolved in deionized distilled water and 95% ethanol (10% ethanol [vol/vol]) and added to the medium to a concentration of 5 μM for 30 min before each experiment. (Ethanol concentration was 0.25% [vol/vol].)

Fluorescence Microscopy

Rhodamine-phalloidin (Molecular Probes Inc., Junction City, OR) was used to label cytoskeletal stress fibers (46). Cells were fixed in 3.7% formaldehyde diluted in PBS for 10 min and then rinsed three times in PBS. Triton X-100 diluted in PBS (0.5% [vol/vol]) was used to permeate the membrane for 5 min, followed by another 5-min rinse in PBS. 10 μl (33 ng) of the rhodamine-phalloidin stock solution was dissolved in 200 μl PBS and used per coverslip. After labeling (20 min, 22°C), the coverslips were washed in PBS, mounted in a 1:1 solution of PBS and glycerol, and observed with an Olympus BTU fluorescence microscope using a 40× UVFL objective. Cells exhibiting well-defined stress fibers with organized arrays spanning across the cell body were scored as "distinct," and those with diffuse patterns were scored as "disrupted." Blind scoring was used to minimize measuring bias.

Chemoluminescence Measurements

The initial batch of aequorin was a gift from Dr. Franklyn G. Prendergast (Mayo Clinic, Rochester, MN) and additional batches were later purchased from Dr. John R. Blinks (Mayo Clinic, Rochester, MN). It was obtained as protein lyophilized from a 1-mg/ml calcium-free buffered solution (150 mM KCl, 5 mM Hepes, pH 7.45) and reconstituted in deionized distilled water containing 10 μM EGTA. All plasticware coming into contact with the protein was sterilized and soaked overnight in sterile 10-mM EGTA solution, then thoroughly rinsed with sterile calcium-free buffered saline (120 mM NaCl, 3 mM Hepes, 0.5 mM EGTA, pH 7.0).

Cells were grown to near confluency in 100-mm culture dishes (~700,000 cells/dish), and aequorin was incorporated by using the scrape-loading technique (26). Briefly, the culture medium was aspirated and the cells were rinsed three times in sterile calcium-free buffered saline at 37°C. The final rinse was removed and 250 μl of the aequorin stock solution (37°C) was added. A sterile rubber policeman was then used to gently scrape the cells, and 2–5 min were allowed to elapse before complete culture medium was added. The scraped cells from one 100-mm culture dish were replated into three 100-mm culture dishes, each containing five acid-washed sterilized glass coverslips (22 × 30 mm) attached to the bottom. The coverslips were taken 18–24 h after plating, at which time the cultures were at a subconfluent stage.

The coverslip containing the cells was sealed cell-side down with vacuum grease onto a 10 × 30 × 1-mm perfusion trough. Various chemicals were presented to the cells through plastic tubing connected to a syringe at a rate of ~0.25 ml/s. A 10 × 40 × 0.1-mm trough was used for electric stimulation to maximize the photoemission area. At 10 V/cm, the current through the trough was ~5.0 mA.

Aequorin chemoluminescence measurements (6) were made by placing the apparatus over the housing of a photomultiplier tube and positioning a mirror directly over the coverslip. A low dark current photomultiplier tube (model R1527; Hamamatsu Corp., Middlesex, NJ) was used to measure low intensity light at the photon counting mode. The setup was enclosed in a light-tight box and the photomultiplier tube was connected through an amplifier/discriminator to a photon counter (model 126; Pacific Instruments, Inc., Concord, CA). The measured luminosity (L) was converted to a free calcium concentration value by calculating the fractional luminescence (L/L_{max}) and using the calibration curve of Allen and Blinks (3). The L_{max} value for each population of aequorin scrape-loaded cells was determined by perfusion with a solution of 2% Triton X-100 and 0.1 M $CaCl_2$, 150 mM KCl, 5 mM Hepes, pH 7.0 (37°C). Since the time course of this L_{max} measurement is slower than when aequorin is suddenly mixed with a saturating free calcium concentration in vitro, a time constant of 0.8 s was used to calculate the peak light intensity (3).

Results

Cell Shape Changes, Preferential Alignment, and Displacement

In an applied electric field (10 V/cm), the cell side facing the cathode exhibited protrusive activity, and many cells showed a displacment of ~1-cell width toward the cathode during a 60-min period. The percentage of spindle-shaped cells increased and these cells preferentially aligned with their long axes perpendicular to the electric field (Fig. 1, *a* and *b*). At progressively lower field strengths, this response became less evident, and at 1 V/cm for up to 2 h, no significant morphological changes were observed (Fig. 2, *a* and *b*). The increase of spindle-shaped cells and preferential orientation was quantitated and presented in our previous works (32,

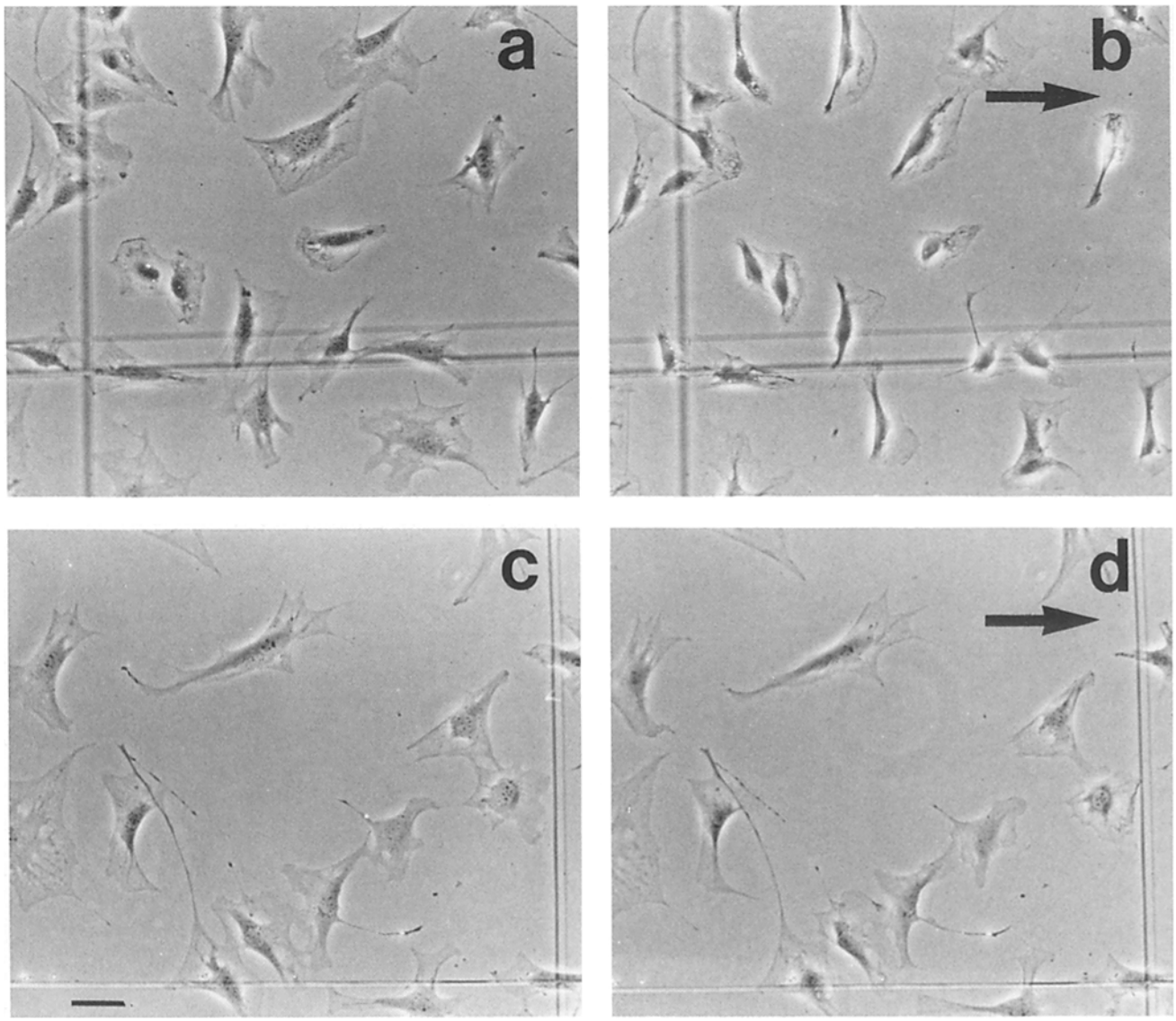

Figure 1. Phase-contrast micrographs of the same fields of view before (*a*) and after (*b*) electric field stimulation in normal buffer; before (*c*) and after (*d*) electric field stimulation in buffer containing 1 μM D-600. Electric stimulatiion was 10 V/cm for 30 min. Arrows indicate field direction. Bar, 50 μm.

47), and similar results were reported by others using different cell types (12, 15, 16, 21, 25, 31, 40). The field-induced cell shape changes, alignment, and positional shifts were not caused by the electroosmotic flow of medium (as shown by perfusion experiments).

The field-induced response is believed to involve calcium flux across the plasma membrane. Electric stimulation in the presence of the calcium channel blocker D-600 blocked the cell shape changes and preferential alignment (Fig. 1, *c* and *d*) in a manner similar to that observed in calcium-depleted buffer or in buffer containing the calcium antagonist lanthanum chloride (32). In media containing D-600, the average speed and the percentage of mobile cells were reduced. Electric stimulation (10 V/cm) under these conditions produced no change in cell mobility with no preferential directional displacement (Table I). Similar responses were observed in the presence of the calmodulin antagonist trifluoperazine, with the average speed of the cells being slightly higher than with D-600 (Table I).

Stress Fiber Disruption

In a normal sparsely populated culture of C3H/10T1/2 fibroblasts, ~85% of the cells exhibit an organized network of actin-containing stress fibers spanning across the cell body (Fig. 3 *a*). Cells incubated with A23187 for 30 min in normal buffer lose the organized stress fiber pattern (Fig. 3 *b*). Electrical stimulation (10 V/cm, 30 min) also results in a disruption of the cytoskeletal network (Fig. 3 *c*), and the threshold for this response seems to start from 1 V/cm (Table II). Cells stimulated for up to 2 h at 1 V/cm are indistinguishable from controls (cells labeled immediately after being taken out of the culture medium or after being incubated for up to 2 h).

Electric stimulation (10 V/cm, 30 min) in calcium-de-

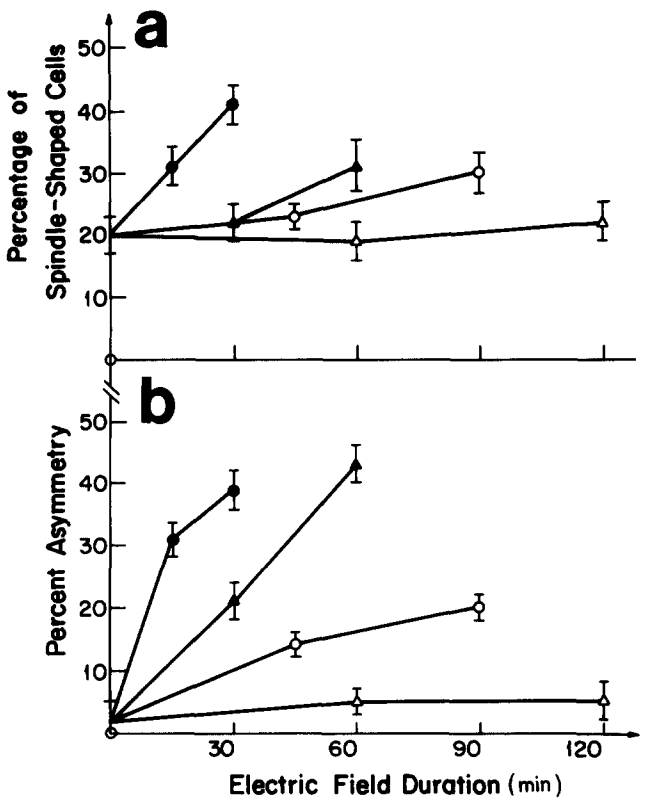

Figure 2. (*a*) The percentage of spindle-shaped cells and (*b*) the percent asymmetry after electric stimulation as a function of field duration. Field strengths were (●) 10 V/cm; (▲) 5 V/cm; (○) 3 V/cm; and (△) 1 V/cm.

pleted buffer, or in buffer containing D-600 or cobalt chloride, resulted in a reduction of the field-induced stress fiber disruption (Table III; Fig. 3 *d*). Incubation with trifluoperazine (30 min, 22°C) caused a slight disorganization of the stress fiber pattern, but in conjunction with the electric stimulation, the anticalmodulin drug also reduced the field-induced disruption. The electric field–induced disruption in the presence of A23187 is similar to that in the absence of the ionophore (Table III). When calcium-depleted buffer or buffer containing cobalt chloride or trifluoperazine was used, the stress fiber disruption caused by the ionophore alone or in conjunction with electric stimulation was not observed. D-600 was not able to inhibit the disruption in ionophore-treated cells.

C3H/10T1/2 fibroblasts preincubated with cytochalasin D exhibited a fragmented stress fiber pattern, and many cells

Table II. Threshold for Stress Fiber Disruption

Stimulation	Duration	Cells scored	Cells with disrupted stress fibers
V/cm	*h*	*n*	%
0	0	256	13 ± 3
0	2	204	16 ± 4
1	2	238	15 ± 3
3	1	243	33 ± 4
5	1	201	52 ± 4
10	0.5	455	87 ± 2

rounded up. When electrically stimulated (10 V/cm, 30 min), the scoring method did not detect any increase in number or preferential orientation of the spindle-shaped cells (results not shown).

Intracellular Free Calcium Measurements

Since the scrape-loading procedure (26) is somewhat harsh (only ~50% of the cells survive immediately after being scraped), the growth of replated scraped populations was measured and compared with cell populations replated by the standard trypsinization procedure. Over a 3-d period, the two populations of cells showed similar growth curves (results not shown). Therefore, the scrape-loading technique had no apparent adverse effects on the subsequent growth of the surviving cells.

Various electric field strengths were applied and the resulting chemoluminescence was measured. Within the limits of instrument sensitivity, significant increases of chemoluminescence were observed only at field strengths >1 V/cm (Fig. 4 *a*). At 3 V/cm, the intracellular free calcium level increases to 1.8 ± 0.1 μM and at 10 V/cm it increases to 4.3 ± 0.2 μM with a response time of ~4 s. Electric stimulation (10 V/cm) in the presence of cobalt chloride or in calcium-depleted buffer does not result in a significant increase of the aequorin signal (Fig. 4 *b*). In the presence of D-600, however, there is a slight increase during stimulation. Therefore, it seems the field-induced increase in intracellular free calcium is not mediated solely by the D-600–binding calcium channels.

When cells are perfused with 4 μM A23187, the intracellular calcium concentration increases transiently to ~10 μM. This increase is significantly reduced when the ionophore is perfused in combination with 10 mM cobalt chloride but not with 1 μM D-600 (results not shown). Thus it seems cobalt chloride can block the ionophore whereas D-600 is selective for the calcium channel.

Table I. Speed and Direction of Movement

Medium	Field strength	Cells scored	Mobile cells	Average speed	Vectorial displacement
	V/cm	*n*	%	*μm/min*	*μm*
Culture media only	0	34	71	0.40 ± 0.0	−3.4 ± 2.8
	10	79	86	0.28 ± 0.02	12.4 ± 1.4
Media + 1 μM D-600	0	61	13	0.03 ± 0.01	1.6 ± 2.8
	10	69	13	0.03 ± 0.01	3.5 ± 3.1
Media + 5 μM trifluoperazine	0	54	24	0.14 ± 0.05	−1.9 ± 3.1
	10	48	29	0.09 ± 0.02	1.4 ± 2.0

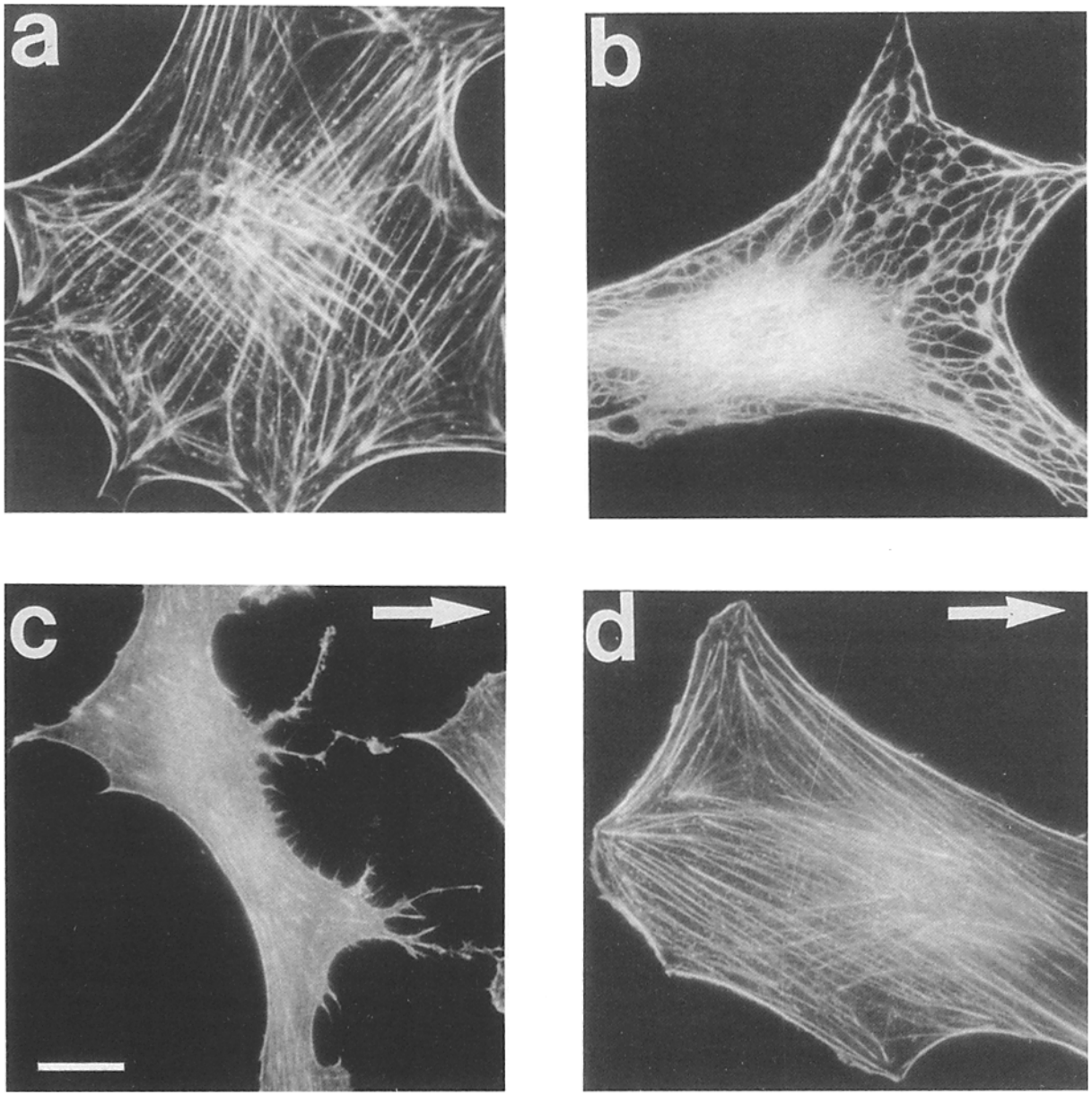

Figure 3. Fluorescence micrographs of cells labeled with rhodamine-phalloidin. Cells incubated (*a*) in normal buffer and (*b*) in buffer containing 4 μM A23187 for 30 min before labeling; and cells stimulated by a 10-V/cm electric field (*c*) in normal buffer and (*d*) in buffer containing 10 mM $CoCl_2$ for 30 min before labeling. Arrows indicate field direction. Bar, 20 μm.

Discussion

Hinkle et al. (21) first observed field-induced cell shape changes and perpendicular alignment using embryonic frog myoblasts. Several other investigators have reported this phenomenon as well as cathode-directed cell migration in frog (12, 40) and quail (15) neural crest cells, embryonic quail (15) and mouse (47) fibroblasts, embryonic frog epithelial cells (25), and embryonic rat osteoblasts (16). The threshold for field-induced shape changes and perpendicular alignment in embryonic quail fibroblasts was measured at ~1 V/cm (15), and this value corresponded to our finding. Our threshold for field-induced disruption of the normal stress fiber organization also started at ~1 V/cm and therefore these two observations could be related. Luther et al. used fluorescently labeled antiactin and reported that in electrically stimulated epithelial cells, the stress fibers became oriented perpendicular to the field, and a band of actin became associated with the lamellae at the cathodal edge and at the ends of the cell (25). Since we can only observe filamentous actin by phalloidin staining, we were not able to observe monomeric actin. Our studies also did not detect any reorientation of stress fibers with respect to the electric field.

Extracellular calcium is required for cell shape changes and movement (18, 27, 28), and antagonists that block calcium flux across the plasma membrane also inhibit cell motility (39). Several researchers have shown that calcium plays a role in field-directed cell shape changes and movement. Migration of ameboid cells toward the cathode was related to the elevated calcium concentration in their tail regions

Table III. Electric Field–induced Stress Fiber Disruption

Conditions		Cells scored	Cells with disrupted stress fibers
		n	%
Normal buffer	Control	939	13 ± 2
	Experiment	455	87 ± 2
Calcium-depleted buffer	Control	327	17 ± 3
	Experiment	400	26 ± 3
Buffer containing 1 μM D-600	Control	163	13 ± 4
	Experiment	280	22 ± 3
Buffer containing 10 mM $CoCl_2$	Control	216	15 ± 3
	Experiment	181	15 ± 3
Buffer containing 5 μM trifluoperazine	Control	192	30 ± 4
	Experiment	244	25 ± 3
In the presence of 4 μM A23187			
Normal buffer	Control	586	65 ± 2
	Experiment	269	89 ± 3
Calcium-depleted buffer	Control	447	14 ± 2
	Experiment	334	22 ± 3
Buffer containing 1 μM D-600	Control	276	70 ± 3
	Experiment	226	84 ± 3
Buffer containing 10 mM $CoCl_2$	Control	210	16 ± 4
	Experiment	200	10 ± 4
Buffer containing 5 μM trifluoperazine	Control	248	23 ± 3
	Experiment	201	29 ± 4

Control, incubation at 22°C for 30 min.
Experiment, 10 V/cm at 22°C for 30 min.

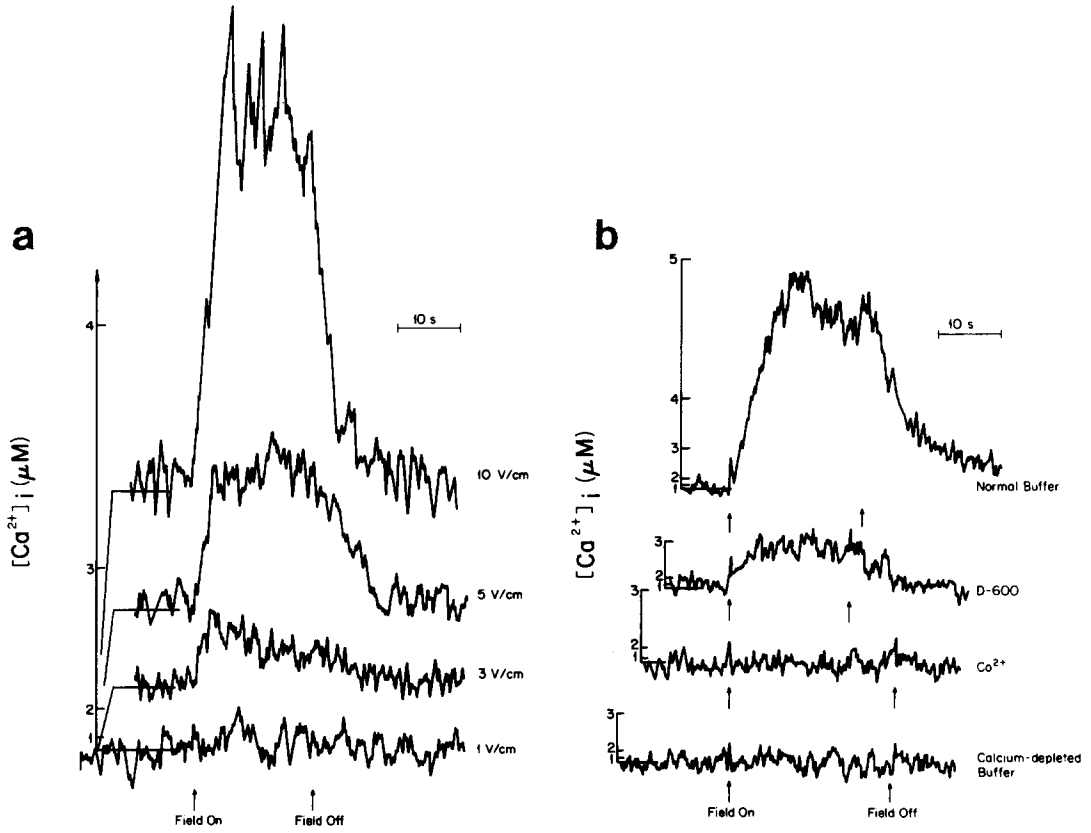

Figure 4. (*a*) The chemoluminescence signal from cells loaded with aequorin and exposed to various electric field strengths. (*b*) The aequorin signal from cells stimulated with 10 V/cm in normal buffer, buffer containing D-600, buffer containing cobalt, and calcium-depleted buffer.

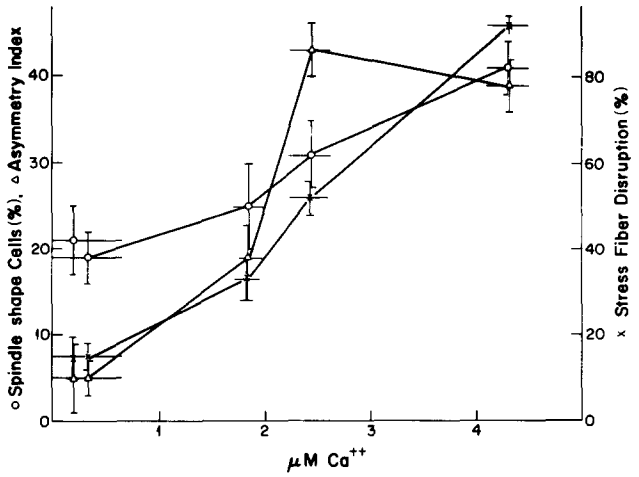

Figure 5. Cell-shape changes, preferential alignment, and stress fiber disruption as a function of intracellular calcium level as measured by aequorin chemoluminescence.

(42). The anode-directed pseudopodial protrusion of macrophages showed a calcium dependence and a lanthanum sensitivity (33). Fish epidermal cell migration toward the cathode was inhibited by calcium antagonists and channel blockers (13, 14). Electric field–induced cell-shape changes and preferential alignment of embryonic mouse fibroblasts were suppressed by reducing calcium influx (32).

Based on the thesis that calcium plays a pivotal role in cellular responses to an external electric field, we correlate our morphological findings with measurements of intracellular free calcium. Fig. 5 graphs the field-induced changes in cell shape and stress fiber organization as functions of field-induced increases in intracellular calcium levels. In this graph the percentage of spindle-shaped cells, asymmetry index, and percent stress fiber disruption data were obtained from electric stimulation experiments using field strengths of 1, 3, and 5 V/cm for 1 h, and 10 V/cm for 30 min (trypan blue exclusion tests indicated significant decreases in viability for 10 V/cm at durations longer than 30 min). Since the amount of aequorin inside each cell is limited and the chemoluminescence induced by calcium binding is irreversible (6), long-term measurement of intracellular free calcium cannot be made by this method. We made the assumption that the initial field-induced intracellular free calcium concentrations measured by aequorin chemoluminescence remained at that level throughout the duration of electric stimulation. The value of 0.2 μM was used for the concentration of cytosolic free calcium in unstimulated cells, a value at the threshold of our measuring system. Other investigators have measured the resting level of intracellular free calcium in fibroblasts using aequorin, and their results ranged from ~0.1 (26) to ~0.3 μM (11).

From Fig. 5 we see that as the field-induced increases in intracellular free calcium rises to the micromolar range, there is a corresponding increase in the percentage of cells with disrupted stress fiber pattern. The percentage of spindle-shaped cells also increases, and these cells are preferentially aligned perpendicular to the electric field.

How does intracellular free calcium modulate cell shape and movement? A 10-V/cm field across a 20-μm-wide cell will result in an ~15-mV drop across the membrane on each side, with a negligible field gradient across the cytoplasm (35). The depolarization on the cathode-facing side may activate voltage-sensitive calcium channels, thus leading to a localized influx of calcium down its concentration gradient. Mittal and Bereiter-Hahn (27) have shown that ionophore-treated epithelial cells in calcium-depleted medium exhibited an enlargement of the leading lamella and directed movement toward a calcium-releasing micropipette. Thus, localized entry of calcium can lead to cell movement as postulated (13, 47).

Actin filament structures and the actomyosin contractile system are two calcium-regulated factors that contribute to cell shape changes and movement (8). In micromolar levels of free calcium, the activities of such nonmuscle actin-binding proteins as α-actinin, vinculin, and gelsolin would result in solation of actin filament structures (45). Thus, the electric field–induced increase of cytosolic free calcium to the micromolar range can account for the field-induced disruption of stress fiber pattern. In nonmuscle cells, the ac-

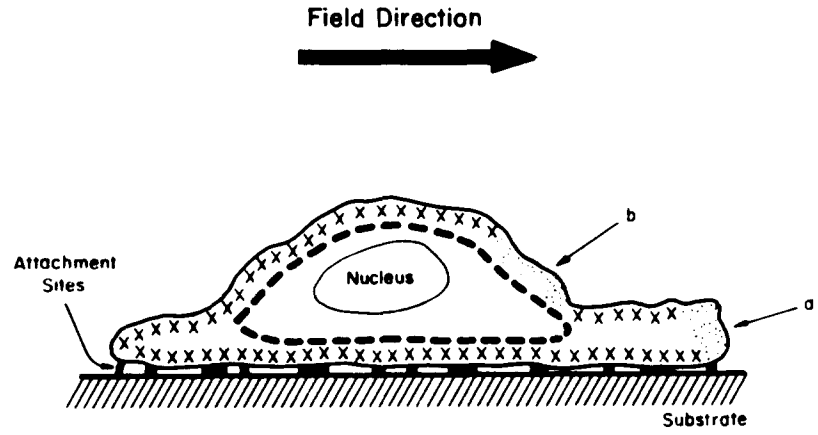

Figure 6. Proposed mechanism for field-directed cell movement. Cross section through a fibroblast in an external electric field. Cross-hatchings represent the cortical actin meshwork. The membrane which encloses the largest span of cytoplasm along the field direction and which is also normal to the field (denoted by *a*) will experience the greatest depolarization of its membrane potential. The area marked *b* will also experience membrane depolarization but to a lesser degree. Calcium influx at these sites will cause depolymerization of the actin cortical meshwork (*dots*). Myosin is located in the cell body region, so at area *b* calcium will also activate the actomyosin system (*bars*). Contraction of the actin cortical meshwork at *b* will increase hydrostatic pressure, and solation of the actin filaments at *a* will increase osmotic pressure. Either one or possibly both of these forces can account for the swelling at *a* due to weakening of its actin cortical meshwork. As the leading edge protrudes forward, new attachment sites are made. The activated actomyosin system at *b* will also pull the cell forward, and the increased tension will cause retraction on the side of the cell facing the anode.

tomyosin contractile system is regulated by calcium through calmodulin activation of myosin light chain kinase (2). Our studies have shown that anticalmodulin drugs inhibit field-induced cell shape changes and perpendicular alignment (32), and reduce cell movement. It seems that the actomyosin contractile system is regulated by field-induced influx of calcium through calmodulin, and that contractile forces are also necessary for cell movement and shape changes (9).

We propose the following model to explain the observed field-induced responses. Since calcium readily binds to intracellular cytoplasmic components, the field-induced entry of calcium into the cytosol through the activated calcium channels will be limited to certain areas of the cell (10). At the edge of the leading lamella facing the cathode (*a* in Fig. 6), calcium entry will result in solation of the cortical actin meshwork. The leading lamella will swell, either because of (*a*) osmotic pressure (34) or (*b*) hydrostatic pressure produced by the cortical actin network at the cell body (5). It will then protrude forward and form new attachment sites (41). The transition area (*b* in Fig. 6) between the leading lamella facing the cathode and the cell body is another area which will experience field-induced local calcium entry. Since myosin was found to be generally located in the cell body region (20), calcium entry here will activate the actomyosin contractile system, thereby pulling the cell forward as well as providing the contractile forces necessary for the hydrostatic pressure mentioned above. The increased tension will cause retraction at the anode-facing side (see Fig. 6).

Our findings suggest that field-directed cell shape changes and alignment are determined by an increase of intracellular free calcium to micromolar levels. The calcium gradient developed by the field-induced influx is believed to influence cytoskeletal reorganization and thereby mediate cathode-directed cell displacement. In C3H/10T1/2 fibroblasts, the threshold for field-induced effects is 1 V/cm. It is interesting to note that when wounds were produced in guinea pig skin, a lateral voltage gradient (gradient parallel to the skin) of >1 V/cm was measured near the wound site (4). Since fibroblasts play an active role in wound repair (17), an electric field gradient can be one of the factors involved in the healing process.

We would like to thank Dr. C. Wenner for his guidance, encouragement, and the use of his cell culture facility. The discussions with Drs. A. Sen and E. Repasky are appreciated. We also thank Drs. F. Sachs and D. Triggle for providing us with the calcium channel blocker D-600, and Dr. F. Prendergast for the aequorin.

This work is supported in part by a grant BC-248 from the American Cancer Society, and by grants GM-28120 and GM-30969 from the National Institutes of Health. Edward K. Onuma received a University Fellowship from the State University of New York at Buffalo and a research support grant from the Graduate Student Association for this work.

Received for publication 6 November 1987, and in revised form 5 February 1988.

References

1. Abercrombie, M. 1982. The crawling movement of metazoan cells. *In* Cell Behaviour. R. Bellairs, A. Curtis, and G. Dunn, editors. Cambridge University Press, Cambridge. 19–48.
2. Adelstein, R. S., and E. Eisenberg. 1980. Regulation and kinetics of the actin-myosin-ATPase interaction. *Annu. Rev. Biochem.* 49:921–956.
3. Allen, D. G., and J. R. Blinks. 1979. The interpretation of light signals from aequorin-injected skeletal and cardiac muscle cells: a new method of calibration. *In* Detection and Measurement of Free Ca^{2+} in Cells. C. C. Ashley and A. K. Campbell, editors. Elsevier/North Holland, Amsterdam. 159–174.
4. Barker, A. T., L. F. Jaffe, and J. W. Vanable, Jr. 1982. The glabrous epidermis of cavies contains a powerful battery. *Am. J. Physiol.* 242: R358–R366.
5. Bereiter-Hahn, J. 1985. Architecture of tissue cells: the structural basis which determines shape and locomotion of cells. *Acta. Biotheor.* 34: 139–148.
6. Blinks, J. R., F. G. Prendergast, and D. G. Allen. 1976. Photo-proteins as biological calcium indicators. *Pharmacol. Rev.* 28:1–93.
7. Borgens, R. B. 1982. What is the role of naturally produced electric current invertebrate regeneration and healing? *Int. Rev. Cytol.* 76:245–298.
8. Buckley, I. K. 1981. Fine-structural and related aspects of nonmuscle-cell motility. *Cell Muscle Motil.* 1:135–203.
9. Burgess, W. H., D. M. Watterson, and L. J. Van Eldik. 1984. Identification of calmodulin-binding proteins in chicken embryo fibroblasts. *J. Cell Biol.* 99:550–557.
10. Campbell, A. K. 1983. Intracellular Calcium: Its Universal Role As Regulator. John Wiley & Sons, Inc., New York. 556 pp.
11. Cobbold, P. H., and M. H. Goyns. 1983. Measurement of the free calcium concentration of single quiescent human fibroblasts before and after serum addition. *Biosci. Rep.* 3:79–86.
12. Copper, M. S., and R. E. Keller. 1984. Perpendicular orientation and directional migration of amphibian neural crest cells in dc electrical fields. *Proc. Natl. Acad. Sci. USA.* 81:160–164.
13. Cooper, M. S., and M. Schliwa. 1985. Electrical and ionic controls of tissue cell locomotion in dc electrical fields. *J. Neurosci. Res.* 13:223–244.
14. Cooper, M. S., and M. Schliwa. 1986. Motility of cultured fish epidermal cells in the presence and absence of direct current electric fields. *J. Cell Biol.* 102:1384–1399.
15. Erickson, C. A., and R. Nuccitelli. 1984. Embryonic fibroblast motility and orientation can be influenced by physiological electric fields. *J. Cell Biol.* 98:296–307.
16. Ferrier, J., S. M. Ross, J. Kanehisa, and J. E. Aubin. 1986. Osteoclasts and osteoblasts migrate in opposite directions in response to a constant electrical field. *J. Cell. Physiol.* 129:283–288.
17. Gabbiani, G., and E. Rungger-Brandle. 1981. The fibroblast. *In* Tissue Repair and Regeneration. L. E. Glynn, editor. Elsevier/North Holland, Amsterdam. 1–50.
18. Gail, M. H., and C. W. Boone. 1971. Effect of colcemid on fibroblast motility. *Exp. Cell Res.* 65:221–227.
19. Harris, A. K. 1983. Cell migration and its directional guidance. *In* Cell Interactions and Development: Molecular Mechanisms. K. M. Yamada, editor. John Wiley & Sons Inc., New York. 123–151.
20. Hegeness, M. H., K. Wang, and S. J. Singer. 1977. Intracellular distribution of mechanochemical proteins in cultured fibroblasts. *Proc. Natl. Acad. Sci. USA.* 74:3883–3887.
21. Hinkle, L., C. D. McCaig, and K. R. Robinson. 1981. The direction of growth of differentiating neurons and myoblasts from frog embryo in an applied electric field. *J. Physiol. (Lond.).* 314:121–135.
22. Jaffe, L. F. 1966. Electrical currents through the developing *Fucus* egg. *Proc. Natl. Acad. Sci. USA.* 56:1102–1109.
23. Jaffe, L. F., and R. Nuccitelli. 1974. An ultrasensitive vibrating probe for measuring steady extracellular currents. *J. Cell Biol.* 63:614–628.
24. Lund, E. J. 1947. Bioelectric Fields and Growth. University of Texas Press, Austin, Texas.
25. Luther, P. W., H. B. Peng, and J. J.-c. Lin. 1983. Changes in cell shape and actin distribution induced by constant electric fields. *Nature (Lond.).* 303:61–64.
26. McNeil, P. L., and D. L. Taylor. 1985. Aequorin entrapment in mammalian cells. *Cell Calcium.* 6:83–93.
27. Mittal, A. K., and J. Bereiter-Hahn. 1985. Ionic control of locomotion and shape of epithelial cells. I. Role of calcium influx. *Cell Motil.* 5:123–136.
28. Moore, L., and I. Pastan. 1979. A calcium requirement for movement of cultured cells. *J. Cell. Physiol.* 101:101–108.
29. Nuccitelli, R. 1983. Transcellular ion currents: signals and effectors of cell polarity. *Mod. Cell Biol.* 2:451–481.
30. Nuccitelli, R. 1986. Ionic Currents in Development. Alan R. Liss, Inc., New York. 375 pp.
31. Nuccitelli, R., and C. A. Erickson. 1983. Embryonic cell motility can be guided by physiological electric fields. *Exp. Cell Res.* 147:195–201.
32. Onuma, E. K., and S-W. Hui. 1985. A calcium requirement for electric field-induced cell shape changes and preferential orientation. *Cell Calcium.* 6:281–292.
33. Orida, N., and J. D. Feldman. 1982. Directional protrusive pseudopodial activity and motility in macrophages induced by extracellular electric fields. *Cell Motil.* 2:243–255.
34. Oster, G. F. 1984. On the crawling of cells. *J. Embryol. Exp. Morphol.* 83(Suppl.):329–364.
35. Poo, M-m. 1981. In situ electrophoresis of membrane components. *Annu. Rev. Biophys. Bioeng.* 10:245–276.
36. Poo, M-m., W-j. H. Poo, and J. W. Lam. 1978. Lateral electrophoresis and diffusion of concanavalin A receptors in the membrane of embryonic muscle cell. *J. Cell Biol.* 76:483–501.
37. Reznikoff, C. A., D. W. Brankow, and C. Heidelberger. 1973. Establish-

ment and characterization of a cloned line of C3H mouse embryo cells sensitive to postconfluence inhibition of division. *Cancer Res.* 33:3231–3238.
38. Robinson, K. R. 1985. The responses of cells to electrical fields: a review. *J. Cell Biol.* 101:2023–2027.
39. Strohmeier, R., and J. Bereiter-Hahn. 1984. Control of cell shape and locomotion by external calcium. *Exp. Cell Res.* 154:412–420.
40. Stump, R. F., and K. R. Robinson. 1983. *Xenopus* neural crest cell migration in an applied electrical field. *J. Cell Biol.* 97:1226–1233.
41. Svitkina, T. M., A. A. Neyfakh, Jr., and A. D. Bershadsky. 1986. Actin cytoskeleton of spread fibroblasts appears to assemble at the cell edges. *J. Cell Sci.* 82:235–248.
42. Taylor, D. L., J. R. Blinks, and G. Reynolds. 1980. Contractile basis of ameboid movement. VIII. Aequorin luminescence during ameboid movement, endocytosis, and capping. *J. Cell Biol.* 86:599–607.
43. Trinkaus, J. P. 1982. Some thoughts on directional cell movement during morphogenesis. *In* Cell Behaviour. R. Bellairs, A. Curtis, and G. Dunn, editors. Cambridge University Press, Cambridge. 471–498.
44. Verworn, M. 1889. Die polare Erregung der Protisten durch den galvanischen Strom. *Pfluegers Arch. Gesante Physiol.* 45:1–36.
45. Weeds, A. 1982. Actin-binding proteins: regulators of cell architecture and motility. *Nature (Lond.).* 296:811–816.
46. Wieland, T., T. Miura, and A. Seeliger. 1983. Analogs of phalloidin. *Int. J. Pept. Protein Res.* 21:3–10.
47. Yang, W-p., E. K. Onuma, and S-w. Hui. 1984. Response of C3H/10T1/2 fibroblasts to an external steady electric field stimulation. Reorientation, shape change, Con A receptor and intramembranous particle distribution and cytoskeleton reorganization. *Exp. Cell Res.* 155:92–104.